IDENTIFICATION OF COHERENT STRUCTURES IN TURBULENT SHEAR FLOWS WITH A FUZZY ARTMAP NEURAL NETWORK

J. FERRE-GINE, R. RALLO, A. ARENAS and FRANCESC GIRALT*
Departament d'Enginyeria Informàtica, Escola Tècnica Superior d'Enginyeria, Universitat Rovira i Virgili, 43006 Tarragona, Catalunya, Spain

Received 12 February 1996
Revised 29 May 1996
Accepted 23 July 1996

An implementation of a Fuzzy Artmap neural network is used to detect and to identify (recognise) structures (patterns) embedded in the velocity field of a turbulent wake behind a circular cylinder. The net is trained to recognise both clockwise and anticlockwise eddies present in the u and v velocity fields at 420 diameters downstream of the cylinder that generates the wake, using a pre-processed part of the recorded velocity data. The phase relationship that exists between the angles of the velocity vectors of an eddy pattern is used to reduce the number of classes contained in the data, before the start of the training procedure. The net was made stricter by increasing the vigilance parameter within the interval [0.90, 0.95] and a set of net-weights were obtained for each value. Full data files were scanned with the net classifying patterns according to their phase characteristics. The net classifies about 27% of the recorded signals as eddy motions, with the strictest vigilance parameter and without the need to impose external initial templates. Spanwise distances (homogeneous direction of the flow) within the centres of the eddies identified suggest that they form pairs of counter-rotating vortices (double rollers). The number of patterns selected with Fuzzy Artmap is lower than that reported for template matching because the net classifies eddies according to the recirculating pattern present at the core or central region, while template matching extends the region over which correlation between data and template is performed. In both cases, the topology of educed patterns is in agreement.

1. Introduction

Wakes have been widely studied in the past because of their fundamental interest and engineering applications (Giralt,[1] Morkovin,[2] Berger and Willie,[3] Laufer,[4] Sarpkaya,[5] Bearman and Graham,[6] Bearman[7] and Griffin[8]). Wake flows offer a wide range of fluid dynamic phenomena that can be conveniently studied in water and wind tunnels, using anemometry and visualisation techniques. Of these phenomena, those related to the structural characteristics of near and far wakes are of uttermost importance for understanding vortex shedding and the role of coherent structures in flow entrainment. Experimental techniques, mainly visualisations and spectral analysis, have been used to characterise structures in the near and far regions of the wake under different flow conditions.

The aim of the present paper is to develop an automatic procedure with a neural network configuration to classify the different structures and large scale motions embedded in two-component velocity signals measured in turbulent flows. Amid these structures vortex-like patterns are of uttermost importance to interpret the dynamics of such flows. Since the implementation of the relationship that exists between the velocity vectors forming the core of an eddy motion is not straight forward with Boolean logic, and

*Departament d'Enginyeria Química.

the amount of data available for training is limited, a Fuzzy ARTMAP Neural Network[9] has been selected to perform the classification of structures. The identification procedure is applied to velocity data measured in the horizontal plane (homogeneous spanwise direction) at the far region of a turbulent wake generated by a circular cylinder. A pre-processing procedure based on the geometric characteristics of the set of vectors representing a vortex-like pattern is proposed to pre-classify eddy motions before data is presented to the net for training.

2. Experimental Details and Dataset Preconditioning

The two-component velocity data used here were measured by Prof. Antonia (University of Newcastle, Australia) at $x/D = 420$ in the wake behind a circular cylinder. These data have been also analysed by Kopp *et al.*[10] using POD and template matching. The experimental conditions of these data are equivalent to those reported by Giralt *et al.*[1] Figure 1(a) shows a portion of the voltage signals sensed by 16

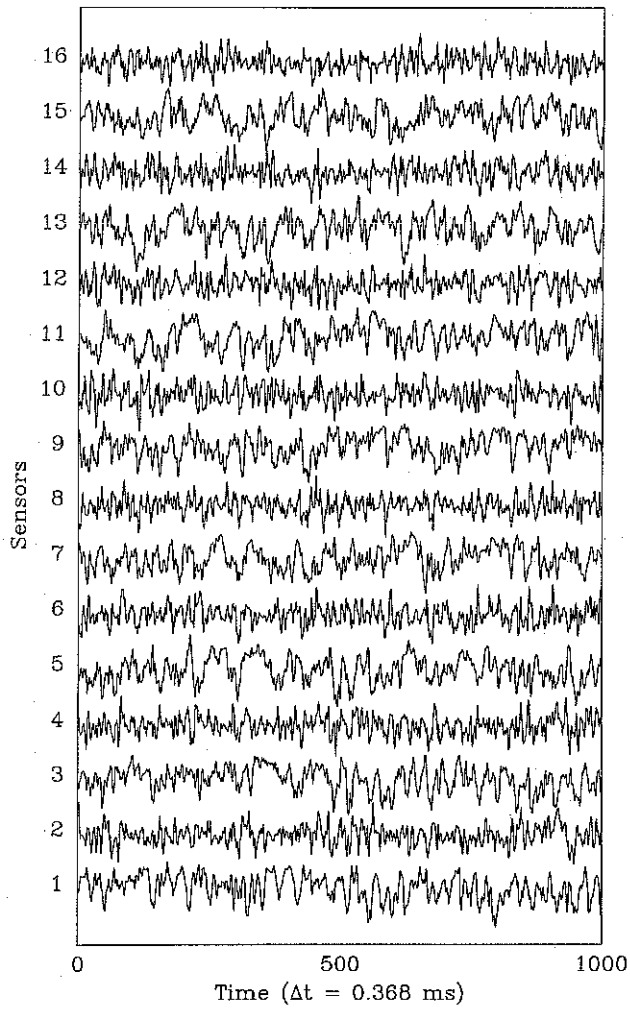

(a)

Fig. 1. (a) Voltage signals of u and v obtained by 16 anemometric channels; (b) velocity field including 54 instants of digitalisation in the horizontal plane of a far wake at $x/D = 420$.

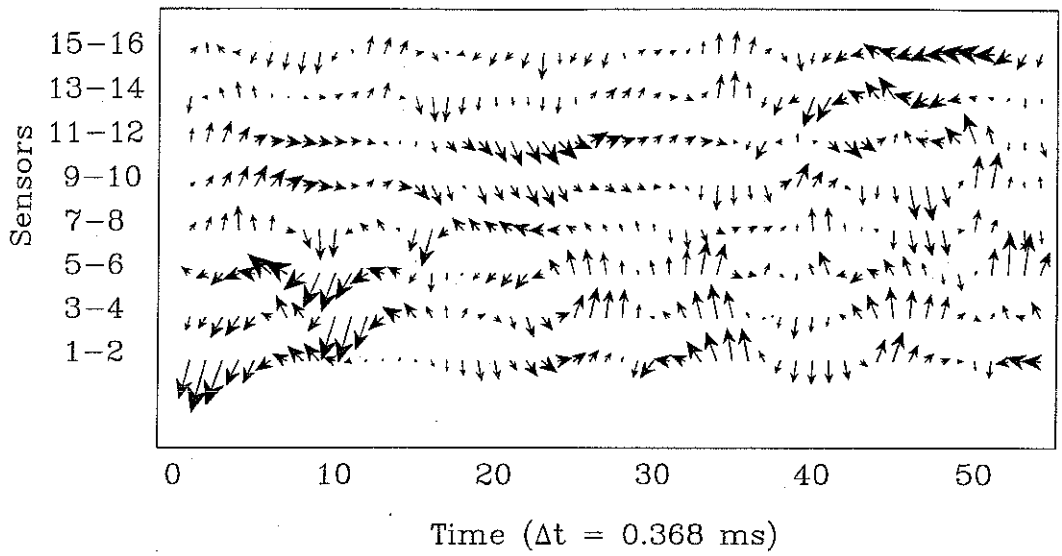

(b)

Fig. 1. (*Continued*)

hot-wire anemometers in the horizontal plane of the wake, and Fig. 1(b) shows the conversion of this signals to velocity vectors.

The objective is to localise vortex-like structures in a highly fluctuating velocity field [see Fig. 1]. The procedure has to be automatic and has to use features of the data only, without any other external information. Pre-processing of data, which is a usual practice in Neural Network field analysis, is inspired in biological behaviour.[11,12] The present pre-processing has two objectives. One is to transform data so that vortical characteristics within frames of velocity data like the one depicted in Fig. 1(b), are enhanced. The other is directed to obtain a good and reduced set of patterns to train the net.

The first step in the pre-processing of data is to transform the velocity field into a field of fluctuating velocities with zero mean. These fluctuations are the only ones analysed here. To obtain a training set and to simplify the final classification procedure, frames F of 3×3 adjacent velocity vectors were considered, and patterns were constructed with the angular components of these vectors. Figure 2 shows the core of a vortical pattern in such a frame. The patterns are represented by normalised velocity vectors (α_1, α_2, α_3, α_4, α_6, α_7, α_8, α_9) within each frame written in

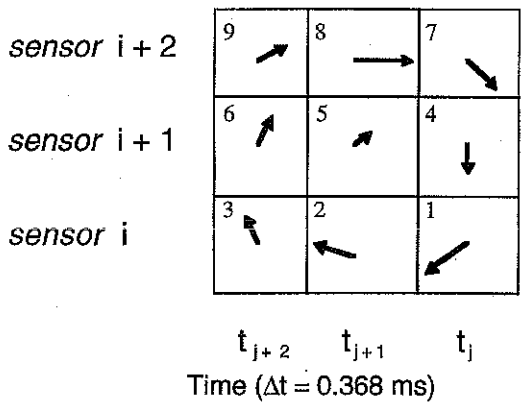

Fig. 2. Representation in a 3×3 frame F of a typical clockwise eddy sensed by three adjacent sensors, located in the spanwise direction of the wake, over three consecutive instants of time.

polar form $m_{1_{\alpha_1}}, \ldots, m_{9_{\alpha_9}}$. The central velocity vector $m_{5_{\alpha_5}}$ is not taken into consideration because the centre of a perfect eddy has zero velocity. A quarter of the pre-processed data, the 20 000 first instants of digitalisation, have been pre-processed to search for the Clockwise (CE) and Anticlockwise (ACE) eddy motions to train the net.

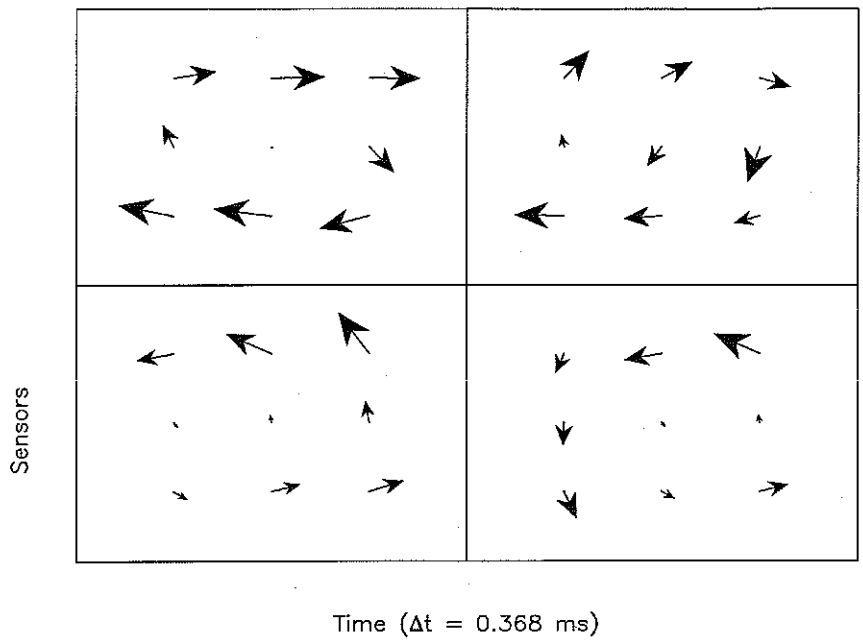

Fig. 3. Four samples of patterns obtained by pre-processing the original velocity signal.

The procedure used to extract good patterns to train the net is as follows. Expressions

$$\alpha_1 \in (\pi/2, 3\pi/2) \text{ and } \alpha_2 \in (\pi/2, 3\pi/2) \text{ and } \alpha_3 \in (\pi/2, 3\pi/2) \quad (1)$$

and

$$\sin \alpha_1 < \sin \alpha_2 < \sin \alpha_3 \quad (2)$$

are used as criteria for identifying CE. Expression (1) establishes that the angular interval of α_1, α_2 and α_3 is the same in a CE. The order of these three vectors in Exp. (2) is invariant under translations. Equivalent expressions for ACE can be written.

The rule that allows the extraction of all frames F representing a CE valid for the training set, consists in fulfilling conditions (1) and (2) when locations 1, 2 and 3 in the frame of Fig. 2 are occupied by different sets of three vectors obtained by rotating the vectors of the frame in a clockwise manner. This rotation sequence ends when all vectors return to their original position. An equivalent procedure is applied to ACE. This process yields 806 frames as a cardinal of the training set, 368 of them corresponding to CE. Figure 3 illustrates four of these frames.

3. The ARTMAP System

The Fuzzy ARTMAP Neural Network[9] is based on the Adaptive Resonance Theory, which avoids the so called stability-plasticity dilema. We have implemented a supervised Fuzzy ARTMAP net for our purposes. This neural network is built with a pair of Fuzzy Art modules,[13] art_a and art_b, linked by an associative memory and a internal controller. The controller is designed to create the minimal number of categories (or hidden units) to meet accuracy criteria. This is done by implementing a learning rule that minimises predictive error and maximises generalisation. Our implementation forces the art_b module to have only two categories: One representing Clockwise Eddies, an the other AntiClockwise Eddies. Another fictitious category considered is the one corresponding to the "I do not know" answer by the net. All inputs that do not pass the reset for a given vigilance ρ_a are included in this category and considered not to be eddy motions. A modification of the learning rule is introduced in our implementation (see Sec. 4). The modified system performs exceptionally well, showing the robustness of Fuzzy

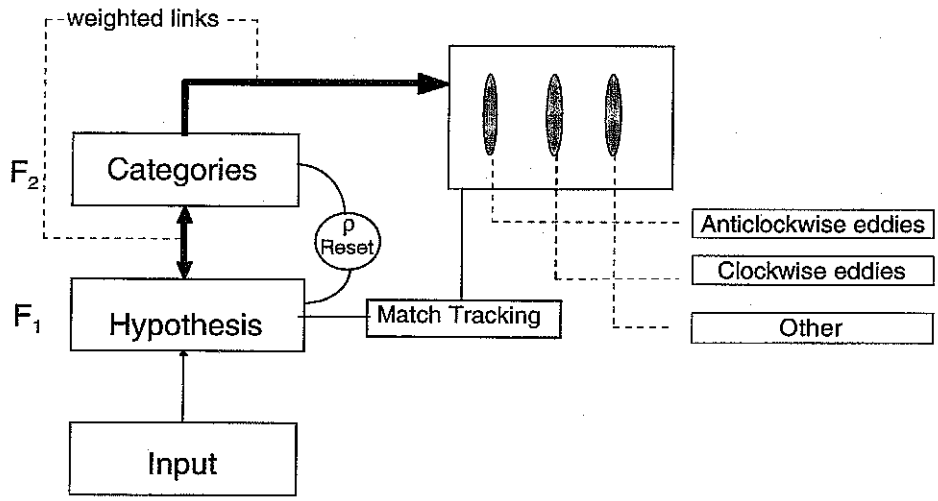

Fig. 4. Sketch of the Fuzzy ARTMAP system.

ARTMAP. A representation of this net is presented in Fig. 4.

Each fuzzy subsystem art_a and art_b includes a field of nodes F_0 which represents a current input vector, F_1. This F_1. receives both bottom-up input from F_0 and top-down input from a field, F_2, which represents the active code or category. The F_1 activity vector is denoted by $\mathbf{x} = (x_1, \ldots, x_M)$, and the F_2 by $\mathbf{y} = (y_1, \ldots, y_M)$. The number of nodes in each field is arbitrary.

Associated with each F_2 category node $j (j = 1, \ldots, N)$ there is a vector $\mathbf{w}_j = (w_{j1}, \ldots, w_{jM})$ of adaptive weights. Initially, when each category is said to be uncommitted,

$$w_{j1} = \cdots = w_{jM} = 1 \tag{3}$$

After a category is selected for coding it becomes committed.

Fuzzy ART dynamics is determined by a choice parameter $\alpha > 0$, a learning rate parameter $\beta \in [0, 1]$, and a vigilance parameter $\rho \in [0, 1]$. For each input $\mathbf{I}$ and F_2 node j, the *choice function* T_j is defined by

$$\mathbf{T}_j(I) = \frac{|I \wedge \mathbf{w}_j|}{\alpha + |\mathbf{w}_j|} \tag{4}$$

In this Eq. (4) the fuzzy AND operator ($\wedge$) is defined by

$$(\mathbf{p} \wedge \mathbf{q}) = \min(p_i, q_i) \tag{5}$$

and the norm $|.|$ by

$$|\mathbf{p}| = \sum_{i=1}^{M} |p_i| \tag{6}$$

for any M-dimensional vectors $\mathbf{p}$ and $\mathbf{q}$. For simplicity, $T_j(\mathbf{I})$ is written as T_j when the input $\mathbf{I}$ is fixed. The system is said to make a *category Choice* when at most one F_2 node can become active at a given time. The category choice is indexed by J, where

$$T_j = \max\{T_j : j = 1, \ldots, N\} \tag{7}$$

When the Jth category is chosen, $y_J = 1$; and $y_J = 0$ for $j \neq J$. In a choice system, the F_1 activity vector $\mathbf{x}$ is characterised by the equation:

$$\mathbf{x} = \begin{cases} \mathbf{I} & \text{if } F_2 \text{ is inactive} \\ \mathbf{I} \wedge \mathbf{w}_J & \text{if the } J\text{th } F_2 \text{ node is chosen} \end{cases} \tag{8}$$

Resonance occurs if the match function $|\mathbf{I} \wedge \mathbf{w}_J|/|\mathbf{I}|$ of the chosen category meets the vigilance criterion

$$\frac{|\mathbf{I} \wedge \mathbf{w}_J|}{|\mathbf{I}|} \geq \rho \tag{9}$$

When the Jth category is chosen, resonance occurs if

$$|\mathbf{x}| = |\mathbf{I} \wedge \mathbf{w}_J| \geq \rho |\mathbf{I}| \tag{10}$$

Learning then ensues, as defined below. Mismatch reset occurs if

$$\frac{|\mathbf{I} \wedge \mathbf{w}_J|}{|\mathbf{I}|} \leq \rho \tag{11}$$

and then a new index J is chosen. The search process continues until the chosen J meets the vigilance criterion (9). Once the search ends, the weight vector $\mathbf{w}_J$ is updated according to equation

$$\mathbf{w}_J^{(new)} = \beta(\mathbf{I} \wedge \mathbf{w}_J^{(old)}) + (1-\beta)\mathbf{w}_J^{(old)} \qquad (12)$$

Fast learning corresponds to $\beta = 1.0$.

art_a and art_b are linked via an inter-ART module, F^{ab}, called a map field. Inputs to art_a and art_b are $\mathbf{I} = \mathbf{A}$ and $\mathbf{I} = \mathbf{B}$, respectively. Variables in art_a or art_b are designated by superscripts a or b. In the former case, for example, $\mathbf{x}^a = (x_1^a, \ldots, x_{2Ma}^a)$ denotes the F_1^a output vector, $\mathbf{y}^a = (y_1^a, \ldots, y_{2Na}^a)$ denotes the F_2^a output vector, and $\mathbf{w}_j^a = (w_{j,1}^a, \ldots, w_{j,2Ma}^a)$ denotes the jthart_a weight vector. For art_b, $\mathbf{x}^b = (x_1^b, \ldots, x_{2Mb}^b)$ denotes the F_1^b output vector, $\mathbf{y}^b = (y_1^b, \ldots, y_{2Nb}^b)$ denotes the F_2^b output vector, and $\mathbf{w}_k^b = (w_{k,1}^b, \ldots, w_{k,2Mb}^b)$ denotes the kth art_b weight vector. For the map field $\mathbf{x}^{ab} = (x_1^{ab}, \ldots, x_{Nb}^{ab})$ denotes the F^{ab} output vector, and $\mathbf{w}_j^{ab} = (w_{j1}^{ab}, \ldots, w_{j2Nb}^{ab})$ denotes the weight vector from the Jth F_2^a node to F^{ab}. Initially, each weight is set equal to 1.

The map field F^{ab} is activated when one of the art_a or art_b categories becomes active. When the Jth F_2^a node is chosen, the input $F_2^a \to F^{ab}$ is proportional to the weight vector w_j^{ab}. When the kth F_2^b is chosen, the F^{ab} node K is activated by 1- to-1 pathways between F_2^b and F^{ab}. If both art_a and art_b are active, as in supervised learning, then F^{ab} activity reflects the degree to which a correct prediction has been made. With fast learning, F^{ab} remains active only if art_a predicts the same category as art_b, via the weight vector $\mathbf{w}_J^{ab}$, or if the active art_a category has not yet learned an art_b prediction. In summary, the F^{ab} output vector $\mathbf{x}^{ab}$ obeys:

$$\mathbf{x}^{ab} = \begin{cases} \mathbf{y}^b \wedge \mathbf{w}_J^{ab} & \text{if the } J\text{th } F_2^a \text{ node is active and } F_2^b \text{ is active} \\ \mathbf{w}_J^{ab} & \text{if the } J\text{th } F_2^a \text{ node is active and } F_2^b \text{ is inactive} \\ \mathbf{y}^b & \text{if } F_2^a \text{ is inactive and } F_2^b \text{ is active} \\ \mathbf{0} & \text{if } F_2^a \text{ is inactive and } F_2^b \text{ is inactive} \end{cases} \qquad (13)$$

If the prediction $\mathbf{w}_J^{ab}$ is disconfirmed by $\mathbf{y}^b$, this mismatch triggers an art_a search for a new category, as follows. At the start of each input presentation, the art_a vigilance parameter ρ_a equals a baseline vigilance $\overline{\rho_a}$. The mapfield vigilance parameter is ρ_{ab}. Match tracking is triggered by a mismatch at the map field F^{ab},

$$|\mathbf{x}^{ab}| < \rho_{ab}|\mathbf{y}^b| = \rho_{ab} \qquad (14)$$

Match tracking increases ρ_a until it becomes slightly larger than the art_a value, $|\mathbf{A} \wedge \mathbf{w}_J^a||\mathbf{A}|^{-1}$. After match tracking,

$$|\mathbf{x}^a| = |\mathbf{A} \wedge \mathbf{w}_J^a| < \rho_a|\mathbf{A}| = \rho_a M_a\,, \qquad (15)$$

When this occurs, the art_a search leads either to ARTMAP resonance, where a newly chosen F_2^a node J satisfies both the art_a matching criterion

$$|\mathbf{x}^a| = |\mathbf{A} \wedge \mathbf{w}_J^a| \geq \rho_a|\mathbf{A}| \qquad (16)$$

and the map field matching criterion

$$|\mathbf{x}^{ab}| = |\mathbf{y}^b \wedge \mathbf{w}_J^{ab}| \geq \rho_{ab}|\mathbf{y}^b| \qquad (17)$$

Otherwise, no such F_2^a node exists, ART search leads to the shutdown of F_2^a for the remainder of the input presentation. Since $w_{ij}^a(0) = w_{jk}^{ab}(0) = 1$ and $0 \leq \rho_a$, $\rho_{ab} \leq 1$, ARTMAP resonance always occurs if J is an uncommitted node.

A learning rule determines how the map field weights w_{jk}^{ab} change through time. During resonance with the art_a category J active, $\mathbf{w}_J^{ab}$ approaches the map field vector $\mathbf{x}^{ab}$. With fast learning, once J learns to predict an art_b category K, that association is permanent, i.e. $w_{JK} = 1$ and $w_{Jk} = 0 (k \neq K)$ for all times. After presentation of all the training samples, the net is ready to undergo a test phase which will show the accuracy of the created categories.

The net was trained for 6 vigilance parameter values in the range 0.9–0.95, obtaining a set of weights for each one. Every net was given, during a test phase, all the possible frames obtained from the full data file, so that all frames with recirculation could be classified.

A modification of the learning rule was used in this implementation of the Fuzzy ARTMAP neural

network. In fast learning, after an association intra-modules was established, weights in both ART modules were updated by the rule

$$\mathbf{w}_J^{new} = (\min(I_1, w_{J_1}^{old}), \ldots, \min(I_N, w_{J_N}^{old})) \quad (18)$$

where J is the committed category. If the vigilance parameter ρ is taken with the maximum value 1.0 then the previous rule becomes

$$\mathbf{w}_J^{new} = \mathbf{I} \quad (19)$$

where I is the presented pattern, and the number of categories equals the number of inputs.

Equation (19) with $\rho < 1.0$, has been used here in the implementation of the net. This rule has the effect of partitioning the training set in a manner that each partition class contains those input patterns committing to the same category. The net becomes stable in the sense that the partition is stable inter two consecutive presentations of the training set, even if the order of the patterns is altered. However, the weights will depend on the last pattern committed to the category. This is consistent because the patterns committing to the same category are very similar. The algorithms used were implemented in FORTRAN 90 codes, which were executed in a CRAY EL'92 computer.

4. Results and Discussion

The net behaves as a human expert, i.e. in addition to sensible choices it commits errors either by excess or default. By excess when it takes as recirculations (vortices) frames which are not, or by default when it refuses frames that are recirculations. This latter situation occurs when the eddy is large and the recirculation appears outside the frame F (3×3). The vigilance parameter is the one that changes the dynamics of the net, making it stricter when it increases in value. The final result corresponds to the intersection of the classification sets that obtained for different values of the vigilance parameter. After intersection, 85% of the frames are shared by all the sets while only 3% belong to just one set. In addition, we have verified that in every frame where Kopp *et al.*[10] confirm, with template matching, a double roller or a pair of counter-rotating eddies, the net classifies two 3×3 frames located nearly side by side in the spanwise direction of the wake, one with a clockwise and the other with anticlockwise eddy. Figure 5 illustrates four of these pairs or double rollers within an extended frame of 8×11 velocity data.

The existence of double rollers or pairs of CE and ACE is confirmed by the fact that, if we take into account a maximum span between eddy centres of 54 sampled points (19.872 ms), a 91% of eddies obtained by the net can be considered as couples and only a 9% as single eddies. Figure 6 shows the proportions between CE and ACE eddies along the whole wake. This proportion tends to 1, reinforcing the idea that eddies mostly occur in pairs.

The net was trained to recognise both CE and ACE eddies in a 3×3 frame of the velocity field. Geometrical properties of the vectors in a frame leads in the fact that the net trained to recognise only CE is able to extract 8 kinds of coherent structures in a turbulent wake, without further training. $S = \{I, s_1, s_2, s_3, s_4, g_{\pi/2}, g_\pi, g_{3\pi/2}\}$ is the group of movements leaving invariant a square.[14] In the group there are four symmetries and four rotations, with $g_{2\pi} = I$.

We have chosen a frame of 3×3 so as to identify the core of eddies present in the wake. Applying this transformations on the vectors in a frame representing a CE, we obtain the following results:

$$\begin{aligned} s_1(\text{CE}) &= \text{Saddle point of type A (SPA)} \\ s_2(\text{CE}) &= \text{Saddle point of type B (SPB)} \\ s_3(\text{CE}) &= \text{Saddle point of type C (SPC)} \\ s_4(\text{CE}) &= \text{Saddle point of type D (SPD)} \\ g_{\pi/2}(\text{CE}) &= \text{Source} \\ g_\pi(\text{CE}) &= \text{ACE} \\ g_{3\pi/2}(\text{CE}) &= \text{Sink} \end{aligned}$$

These events and the CE are depicted in Fig. 7. The relationship between the four saddles and the CE in Fig. 7 confirms previous turbulence studies in the sense that searching for saddles is appropriate to identify eddies in three-dimensional flows.

The movements s_1, s_2, s_3, s_4, g_π have order two in the group so they are inverses of themselves, while $g_{\pi/2}$, $g_{3\pi/2}$ are mutually inverse. The rotations are also a subgroup of fourth order and each symmetry with the identity movement being a subgroup of second order. Hence several procedures can be followed

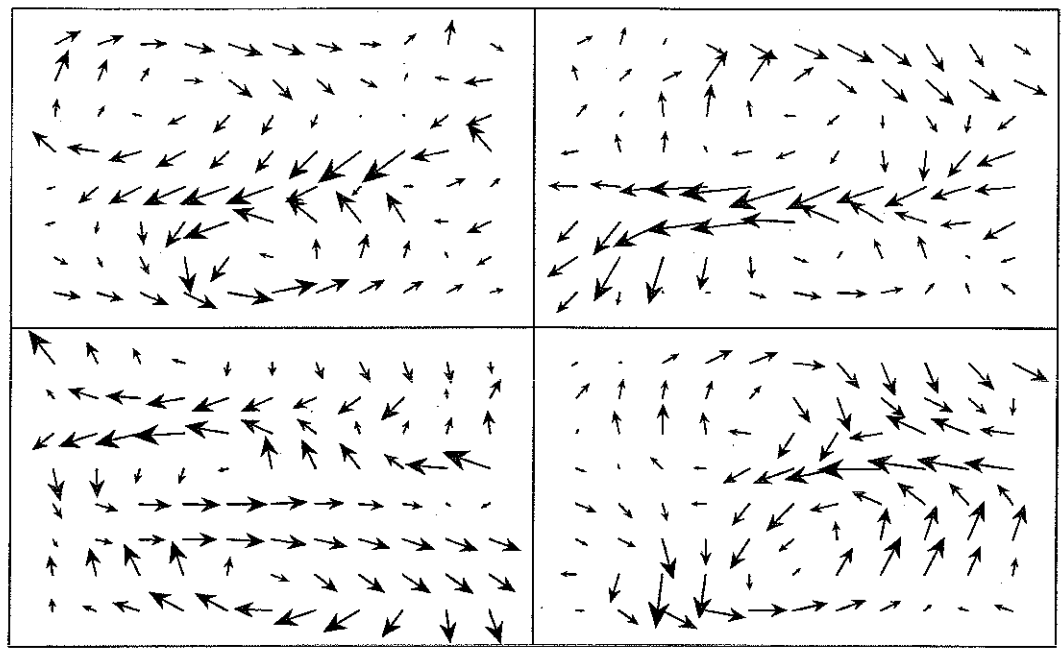

Fig. 5. Visualisation of four double rollers classified, with a Clockwise Eddy (CE) at the top and an Anticlockwise Eddy (ACE) at the bottom.

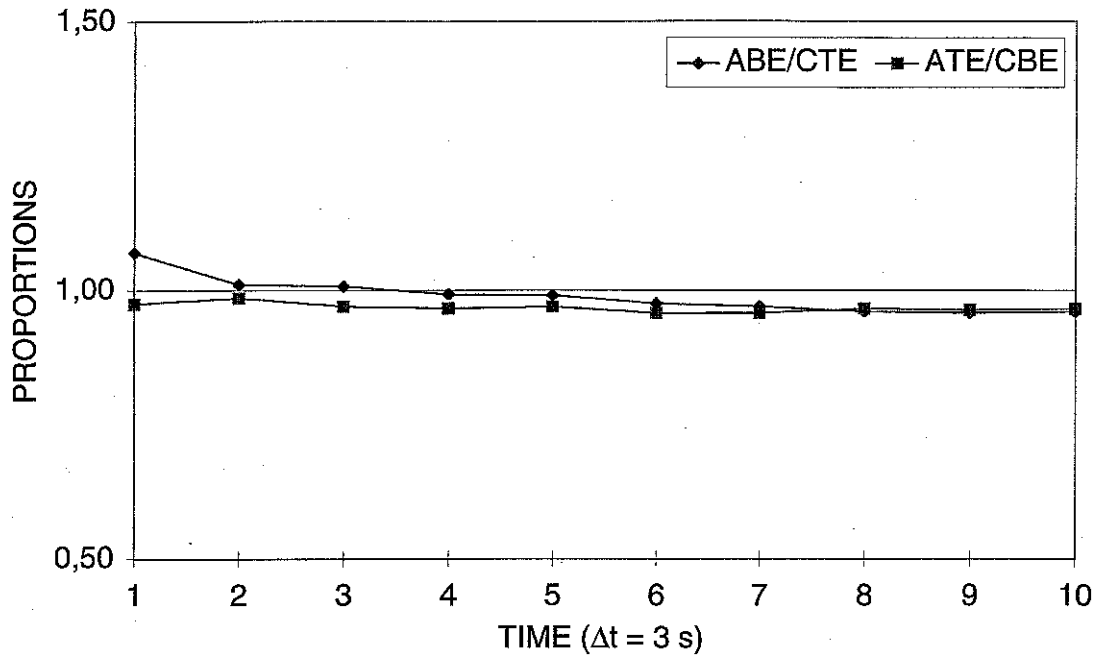

Fig. 6. Proportions between TAE and BCE, and BAE and TCE. Here A ≡ anticlockwise; C ≡ clockwise; B ≡ the first four sensors; T ≡ the last four sensors; E ≡ eddy.

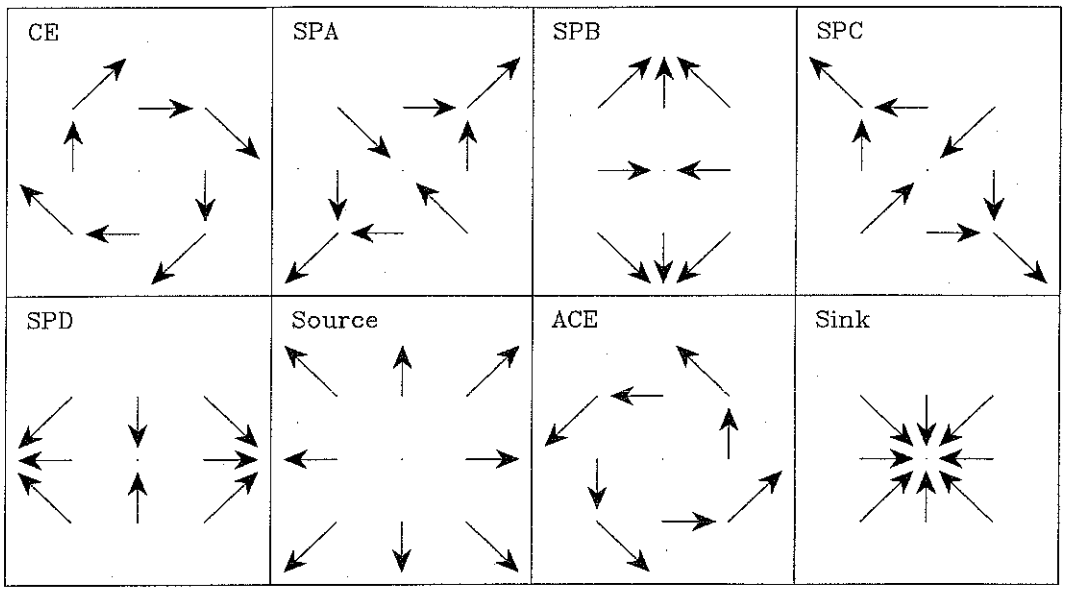

Fig. 7. Transformation of a CE under the S group.

to identify all these structures. One of these procedures consists in the following steps:

(i) The net is trained to recognise CE;
(ii) the net extracts the CE from the data;
(iii) all frames extracted as CE are discarded from the velocity field;
(iv) the remaining original data is transformed by g_π.

Steps (ii), (iii) and (iv) are iterated, changing the transformer movements sequentially so that the remaining structures are obtained according to

$$g_\pi \rightarrow \text{ACE}$$
$$s_1 \rightarrow \text{SPA}$$
$$s_2 \rightarrow \text{SPB}$$
$$s_3 \rightarrow \text{SPC}$$
$$s_4 \rightarrow \text{SPD}$$
$$g_{\pi/2} \rightarrow \text{Sinks}$$
$$g_{3\pi/2} \rightarrow \text{Sources}$$

This procedure can be altered, using information about the nature of the wake to speed program execution. Using the fact that the movements are elements of a group, it is possible to transform data without going back to the original at the end of each transformation. For instance, applying the movements I, g_π, s_3, $g_{\pi/2}$, $g_{\pi/2}$, $g_{\pi/2}$, s_1, g_π in this order, the results are equivalent to those obtained from the procedure above. Presently, a derived kind of ART system called Fusion ARTMAP[15] is being implemented because it saves time in the pre-processing and classification of data.

5. Conclusions

A Neural System based on Fuzzy ARTMAP has been successfully applied to recognise coherent structures in the velocity field of a turbulent wake without the need to use initial external template patterns. The eddy patterns obtained corroborate the results reported in previous pattern recognition analysis. In the present study 27% of the signal is classified as eddies having a minimum size of 3×3 vectors in the matrix of data. Most of these vortices are paired to another eddy with opposed rotation, in agreement with previous pattern recognition analysis based on template matching. Thus the Fuzzy ARTMAP system is a good classifier for multi-sensor patterns. Present results also suggest that searching for saddle points

may be the best choice to classify structures in three-dimensional turbulent flows.

Acknowledgments

We give our thanks to Prof. R. A. Antonia for providing his experimental data. We also wish to thank Professor Gail Carpenter and Dr. Yousif Asfour for their comments on ART. The experimental support of J. A. Ferre is also greatly appreciated. Financial support was provided by DIGICYT project PB93-0656-C02-01.

References

1. F. Giralt and J. A. Ferré 1983, "Structure and flow patterns in turbulent wakes," *Physics Fluids*, **A5**, 1783–1789.
2. M. V. Morkovin 1964, "Flow around a circular cylinder — A kaleidoscope of challenging fluid phenomena," in *ASME Symposium on Fully Separated Flows*, ed. A. G. Hansen (ASME, New York), p. 102.
3. E. Berger and R. Willie 1972, "Periodic flow phenomena," *Annu. Rev. Fluid Mech.* **14**, 313.
4. J. Laufer 1975, "New trends in experimental turbulence research," *Annu. Rev. Fluid Mech.* **7**, 307.
5. T. Sarpkaya 1979, "Vortex-induced oscillations," *J. Appl. Mech.* **46**, 241.
6. P. W. Bearman and J. M. R. Graham 1980, "Vortex shedding from bluff bodies in oscillatory flow: A report on Euromech 119," *J. Fluid Mech.* **99**, 225.
7. P. W. Bearman 1984, "Vortex shedding from oscillating bluff bodies," *Annu. Rev. Fluid Mech.* **16**, 195.
8. O. M. Griffin 1985, "Vortex shedding from bluff bodies in a sheer flow," *J. Fluids Eng.* **107**, 298.
9. G. A. Carpenter, S. Grossberg, N. Marcuzon, J. H. Reinolds and D. B. Rosen 1992, "Fuzzy ARTMAP: A neural network architecture for incremental supervised learning of analog multidimensional maps," *IEEE Trans. on Neural Networks* **3**, 698–713.
10. G. Kopp, J. A. Ferre and F. Giralt 1995, "A hybrid pattern-recognition and proper orthogonal decomposition technique for identifying the average structure in turbulence," *Submitted to the ASME J. Fluids Eng.*
11. B. Fisher 1973, "Overlap of receptive field centres and representation of the visual field in the cat's optic tract," *Vision Res.*, **13**, 2113.
12. E. L. Schwarz, "Spatial mapping in the primate sensory projection: Analytic structure and relevance to perception," *Biol. Cybern.* **25**, 781.
13. G. Carpenter, S. Grossberg and D. Rosen 1991, "Fuzzy ART: Fast stable learning and categorization of analog patterns by an adaptive resonance system," *Neural Networks* **4**, 759–771.
14. R. Shaw 1983, "Multilinear algebra and group representations," Vol. II of *Linear Algebra and Group Representations* (Academic Press, London).
15. Y. Asfour 1995, "Fusion ARTMAP: Neural Networks for multi-sensor fusion and classification," Ph.D. Thesis, Boston University.